



Cite this: *Chem. Commun.*, 2020, **56**, 14463

Received 2nd September 2020,
Accepted 27th October 2020

DOI: 10.1039/d0cc05939k

rsc.li/chemcomm

Ratiometric Raman spectroscopy represents a novel sensing approach for the detection of fluoride anions based on alkyne desilylation chemistry. This method enables rapid, anion selective and highly sensitive detection of fluoride in a simple paper-based assay format using a portable Raman spectrometer.

Raman microscopy is a powerful method for chemical analysis and biological imaging because it provides a spectral fingerprint with chemical specificity in a non-destructive manner.¹ An emerging approach for chemical sensing is alkyne-tag Raman imaging (ATRI) which has enabled *in situ* biomolecular detection with high sensitivity, and multiplex analysis using low molecular weight Raman labels and sensor moieties.² Alkynes have discrete vibrational modes within the cellular-silent region of the Raman spectrum (1800–2800 cm⁻¹) which greatly facilitates their detection in biological samples.³ Early examples of ATRI reported metabolic labelling of intracellular biomolecules with alkyne-labelled precursors for the detection of nascent DNA,⁴ glycans⁵ and proteins⁶ amongst others. Since then, functionalisation of small molecules with alkyne labels has enabled the intracellular visualisation of drugs,⁷ natural products^{8,9} and lipids¹⁰ using Raman and stimulated Raman scattering (SRS) microscopy.

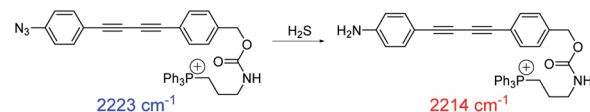
An unexplored application of ATRI is the development of small molecule sensors for the detection and quantification of endogenous chemicals, ions and biomolecules. Two isolated examples make use of oligoyne scaffolds for intracellular hydrogen sulphide

sensing¹¹ and for pH quantification¹² (Fig. 1). In each of these reports, the ratiometric Raman sensor relies on analyte-induced changes of the sensing group resulting in a change in the Raman shift and/or scattering properties of the alkyne moiety. As such, ratiometric sensing approaches are advantageous because there is an effective internal referencing that increases sensitivity and improves quantification.^{13,14}

Fluoride is a biologically important anion that is readily absorbed by the body but is excreted slowly, and as such, over-exposure to fluoride may result in gastric and kidney problems, bone diseases and fluorosis.¹⁵ There has been much interest in the development of fluorescence-based sensors for fluoride detection (Fig. S1, ESI[†]),¹⁶ notably, using the fluoride-mediated desilylation of Si–O groups^{17–19} and Si–C (alkyne) groups^{20–26} as prominent examples for military and cellular applications.

Despite 20 years of developing fluorescent fluoride sensors based on Si–F chemistry, significant challenges have been

Previous work: H₂S sensing (Ref. 11)



identified.²⁷ First, the structural complexity of fluorescent sensors increases the synthetic effort and expense required to prepare the sensors, restricting translation to low-cost, in-field applications. Second, the use of fluorophores that are not compatible with NIR excitation, which is essential for biological compatibility due to reduced photodamage and enhanced imaging depth penetration. Third, the requirement of a surfactant (e.g. cetyltrimethylammonium bromide, CTAB) to enable detection in organic–aqueous solvent mixtures, once again restricting translation.²⁸ Here we propose the use of Raman spectroscopy as a novel method to address these limitations; an extremely small ratiometric sensor molecule (<200 Da) is used to detect fluoride with NIR excitation in aqueous mixtures without the use of a solubilising agent (Fig. 1). Our method enables rapid monitoring of fluoride ions in solution and in a test-paper assay.

To test the validity of a Raman-based approach to detect fluoride ions, we chose to study the fluoride-mediated desilylation of alkyne groups as a model reaction.²⁹ Raman spectroscopy is well-suited to temporal monitoring of chemical reactions in a non-destructive manner,³⁰ in particular, for reactions of alkynes.³¹ The cleavage of Si–C alkyne bonds by fluoride is rapid and irreversible owing to the significant differences in the bond dissociation energies (Si–C $\sim 290 \text{ kJ mol}^{-1}$; Si–F $\sim 590 \text{ kJ mol}^{-1}$).¹⁵ We designed 4-((trimethylsilyl)ethynyl)benzonitrile **1** as an extremely simple molecular Raman sensor, which incorporated two bioorthogonal Raman groups and was readily synthesised in high yield (95%) in a single step from commercially available starting materials (see ESI† for details). The reaction of **1** (50 mM) with tetra-*n*-butylammonium fluoride (TBAF, 1 equiv.) in THF resulted in complete desilylation of the alkyne group within 1 minute (thus forming compound **2**), and resulted in a red-shifting of the alkyne stretching frequency from 2162 cm^{-1} to 2109 cm^{-1} (Fig. 2). This observation is consistent with the Raman spectra of the neat compounds (Fig. S2, ESI†).

We proposed that, based on the 53 cm^{-1} shift in the alkyne frequency, ratiometric sensing could be achieved to confirm the presence of fluoride ions in solution. Furthermore, upon the removal of the silyl group, there was a marginal shift in the nitrile peak ($2231 \text{ cm}^{-1} \rightarrow 2230 \text{ cm}^{-1}$) which offers a second motif for ratiometric sensing. In addition, the relative intensity of the phenyl $\text{C}=\text{C}$ peak ($\sim 1600 \text{ cm}^{-1}$) decreased upon desilylation, which is consistent with the relative peak intensities in the Raman spectra of the solid samples. To demonstrate the versatility of this approach, we showed that desilylation of sensor **1** was also successful using inorganic fluoride sources, including NaF and CsF in a THF:water (1 : 1 v/v) mixture (Fig. S3, ESI†).

A series of control reactions were followed by Raman spectroscopy and validated using UV-visible spectrometry. Fig. S4A demonstrates the control reaction of sensor **1** in the absence of fluoride which showed no change in the Raman spectra over 30 min. In addition, no reaction was observed upon addition of a range of different TBA^+ and Na^+ counter anions (Fig. S4B–D (ESI†) respectively). The sensor is, however, unstable at high pH ($>\text{pH } 10$, Fig. S4E, ESI†) and in the presence of NaI, which is consistent with observations of previous sensors of this type.²⁰ Fig. S5A (ESI†) shows that the

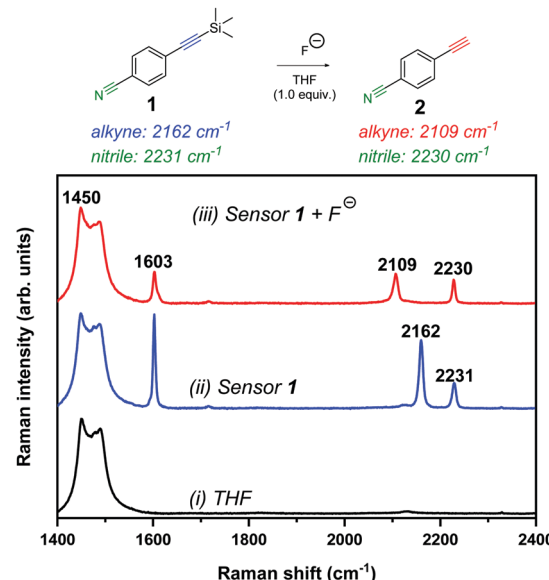


Fig. 2 Raman spectral analysis of the desilylation reaction of sensor **1**. Raman spectrum of (i) THF solvent, (ii) sensor **1** (50 mM) in THF and (iii) sensor **1** (50 mM) + TBAF (50 mM) in THF (spectrum acquired <1 min after TBAF addition). Spectra were acquired using 785 nm laser excitation for 10 s with a 5× objective lens ($\sim 180 \text{ mW}$). The spectra are normalised to the intensity of the peak at 1450 cm^{-1} . The following peak annotations have been included for clarity: 1450 cm^{-1} (THF CH_2 def.);³² 1603 cm^{-1} ($\text{C}=\text{C}$ phenyl); 2109 cm^{-1} ($\text{C}\equiv\text{C}$ of desilylated compound, **2**); 2162 cm^{-1} ($\text{C}\equiv\text{C}$, sensor **1**) and $2230/2231 \text{ cm}^{-1}$ ($\text{C}\equiv\text{N}$; sensor **1** and compound **2**).

detection limit of sensor **1** in solution using Raman spectroscopy is $\sim 250 \mu\text{M}$, enabling sensitive detection of fluoride in solution (Fig. S5B, ESI†), whilst Fig. S5C (ESI†) shows the reaction proceeds in THF: phosphate buffer (1 : 1 v/v) mixture. UV-visible spectrometry showed a reduction of the λ_{max} at $\sim 280 \text{ nm}$ upon addition of fluoride, which is in close agreement with related trimethylsilyl-protected alkyne sensors (Fig. S6, ESI†).²⁰ Together, these data indicated the potential for extremely rapid and sensitive detection of fluoride in organic solution using Raman spectroscopy.

It is desirable to detect fluoride in aqueous solutions for use in analysis of groundwater and drinking water samples, although the majority of fluorescent sensors have only been examined in neat organic medium.²⁸ Water is only weakly Raman active, and therefore, generates minimal interference in Raman analysis.¹ Having established the detection of fluoride anions by **1** in organic solvents, we examined our system in aqueous mixtures. We repeated the reaction monitoring experiments with sensor **1** (50 mM) using an increased [TBAF] (75 mM, 1.5 equiv.) to compensate for the high enthalpy of hydration of fluoride in water ($\Delta H = -504 \text{ kJ mol}^{-1}$).³³ Upon addition of excess fluoride to the reaction mixtures, Raman spectra were recorded every 0.5 s for rapid detection. The peak intensities of the starting material (2162 cm^{-1}), the desilylated product (2109 cm^{-1}) and the nitrile band ($2230\text{--}2231 \text{ cm}^{-1}$) were plotted as a function of time as the water content of the mixture was varied from 0–25% (v/v). Fig. 3A shows a representative example of a reaction conducted in 25% water in THF and indicates the desilylation reaction was extremely



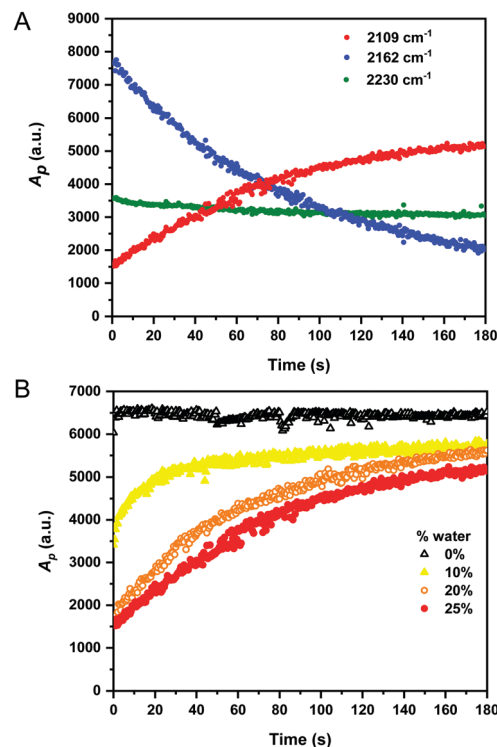


Fig. 3 Time-resolved analysis of the desilylation reaction of sensor **1** in aqueous/organic mixtures. (A) A mixture of sensor **1** (50 mM) and TBAF (75 mM) in THF:water (75 : 25 v/v) was prepared and Raman spectra were acquired after \sim 5 s following TBAF addition. Raman spectra were acquired continuously using 785 nm laser excitation for 0.5 s using a 5 \times objective lens (\sim 180 mW) and normalised to the intensity of the THF solvent peak at 1450 cm^{-1} (CH_2 def.). The peak areas (A_p) at 2162 cm^{-1} ($\text{C}\equiv\text{C-TMS}$), 2109 cm^{-1} (desilylated alkyne) and $2230\text{--}2231\text{ cm}^{-1}$ ($\text{C}\equiv\text{N}$) are plotted as a function of time. (B) Analysis of the desilylation of sensor **1** (50 mM) using TBAF (75 mM) as the % water in THF for the reaction mixture is varied (0–25%). A_p is peak area at 2109 cm^{-1} plotted as a function of time for the different initial % water. Raman spectra were acquired using identical conditions to A.

rapid, with the formation of desilylated product over the course of the experiment (\sim 90% completion at 180 s). Similar plots for the other conditions are provided in Fig. S7 (ESI ‡). Interestingly, the peak area for the nitrile band at $\sim 2231\text{ cm}^{-1}$ also varied throughout the reaction time course, confirming that the desilylation of the alkyne group significantly influenced the electronic properties of the benzonitrile group. Fig. 3B presents the integrated peak areas for the desilylated product at 2109 cm^{-1} as a function of time when the reaction was performed using different initial % water. As the water content of the reaction mixture increased, the rate of product formation decreased. This was likely due to the hydration enthalpy of fluoride in water. 33 In spite of this, these results indicate an extremely fast response time (< 20 s) for fluoride detection in aqueous–organic mixtures which compares favourably to most fluorescent sensors.

We next sought to assess the application of Raman sensor **1** on different materials to demonstrate the versatility of the approach. Recently, the use of paper-based substrates for fluoride sensing with a fluorescent probe has been reported. 34 To demonstrate the application of Raman spectroscopy in this area, we pre-treated

filter paper test strips with sensor **1** (10 μL of 100 mM solution in THF) which were air-dried for 5 minutes before a 300 μL solution of TBAF in THF (0.125–5 mM) was applied directly onto the paper. Raman maps ($20\text{ }\mu\text{m} \times 20\text{ }\mu\text{m}$; 400 individual spectra) were acquired across the sample test strip after drying (\sim 2 minutes). Representative Raman maps and average Raman spectra from the maps are presented in Fig. 4. As the fluoride concentration increased, so too the ratio of $2105/2160\text{ cm}^{-1}$ (alkyne **2**/alkyne **1**) increased, and the ratio $2231/2237\text{ cm}^{-1}$ (nitrile **2**/nitrile **1**) arising from the benzonitrile group also increased (ratiometric images provided in Fig. S8 (ESI ‡) and additional repeat in Fig. S9, ESI ‡). Interestingly, the Raman shift of the alkyne and nitrile group of the sensor **1** were slightly shifted when analysed on paper (2160 and 2237 cm^{-1}) when compared to solution phase analysis (2162 and 2231 cm^{-1}), potentially due to differences in local intramolecular bonding in solution compared to solid-phase. Using this simple ratiometric approach, fluoride detection at concentrations as low as 125 μM could be achieved (Fig. 4 and Fig. S8, ESI ‡) which compares favourably to a recently reported colorimetric sensor (5.75 mg L^{-1} , $\sim 300\text{ }\mu\text{M}$ in 3 : 7 v/v EtOH : water) 35 and a coordination-based sensor ($300\text{ }\mu\text{M}$ in aqueous buffer). 36 In addition, we found that our low-cost paper-based sensing system was compatible with handheld, portable Raman detection (Fig. S10, ESI ‡), which demonstrates a potential translation of this method for in-field fluoride analysis. Together, these results highlight ratiometric Raman spectroscopy as a novel detection method for fluoride ions in solution using a simple paper-based assay format.

Compound **1** represents an extremely low molecular weight chemical sensor for fluoride detection which works using NIR excitation for ratiometric Raman spectroscopy. Advantages of NIR excitation are biological compatibility and operator safety, particularly given that many fluorescent sensors require cell-damaging

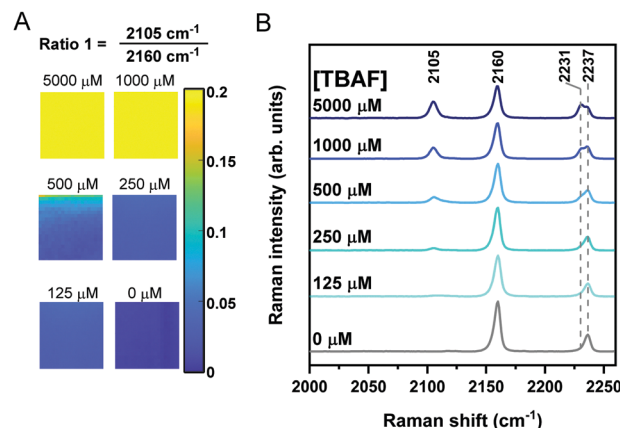


Fig. 4 Paper-based detection of fluoride using Raman sensor **1**. (A) Filter paper was pre-treated with sensor **1** (100 mM in THF, 10 μL) before air-drying and subsequent direct addition of TBAF in THF (300 μL) at the indicated concentrations. Raman maps were acquired across $20\text{ }\mu\text{m} \times 20\text{ }\mu\text{m}$ (1 μm pixel size; 400 spectra) using 785 nm laser excitation with a 20 \times objective lens (\sim 180 mW) for 0.5 s. The maps represent the ratio $2105\text{ cm}^{-1}/2160\text{ cm}^{-1}$. For the blank sample, 10 mM TBACl replaced TBAF. (B) Average Raman spectra from maps presented in A. Peak annotations are in cm^{-1} .

UV excitation.¹⁵ The narrow resonances of Raman peaks ($\sim 40\text{ cm}^{-1}$) enables clear, unambiguous and fully resolved detection of the starting material and product in a single Raman spectral acquisition. This represents a significant advantage to the “turn-on” fluorescent probes which are currently reported, as typically only the desilylated product generates a fluorescent signal. Furthermore, the narrow resonances of Raman shifts are advantageous over ratiometric fluorescent sensors, which typically have broad emission profiles ($\sim 1500\text{ cm}^{-1}$), imposing a limit on the multiplexing capability of the sensing system.³⁷

The detection of the alkyne sensor in solution and on test paper strips highlights the versatility of Raman spectroscopy for small-molecule sensor detection. Our results indicate that fluoride concentrations as low as $125\text{ }\mu\text{M}$ generate a ratiometric output in our simple paper-based assay. This is below the level at which biological toxicity was observed in cells (extracellular $[\text{NaF}] = 3\text{ mM}$)³⁸ and is within the maximum contaminant level defined by the U.S. Environmental Protection Agency (4.0 mg L^{-1} , $211\text{ }\mu\text{M}$).³⁶ We anticipate that the limit of detection of our sensing method could be improved by increasing the Raman scattering intensity of the alkyne sensor through conjugation to form a poly-yne,² whilst different silicon capping groups could be investigated as alternative sensing motifs for improved pH stability in alkaline solutions.²⁰

We thank the University of Strathclyde, the EPSRC and GlaxoSmithKline for financial support. The research data associated with this paper will become available from the University of Strathclyde at the following link: <https://doi.org/10.15129/46582865-502a-43be-907f-bdc41032be1e>.

Conflicts of interest

There are no conflicts to declare.

Notes and references

- 1 W. J. Tipping, M. Lee, A. Serrels, V. G. Brunton and A. N. Hulme, *Chem. Soc. Rev.*, 2016, **45**, 2075–2089.
- 2 H. Yamakoshi, K. Dodo, A. Palonpon, J. Ando, K. Fujita, S. Kawata and M. Sodeoka, *J. Am. Chem. Soc.*, 2012, **134**, 20681–20689.
- 3 A. F. Palonpon, M. Sodeoka and K. Fujita, *Curr. Opin. Chem. Biol.*, 2013, **17**, 708–715.
- 4 H. Yamakoshi, K. Dodo, M. Okada, J. Ando, A. Palonpon, K. Fujita, S. Kawata and M. Sodeoka, *J. Am. Chem. Soc.*, 2011, **133**, 6102–6105.
- 5 S. Hong, T. Chen, Y. Zhu, A. Li, Y. Huang and X. Chen, *Angew. Chem., Int. Ed.*, 2014, **53**, 5827–5831.
- 6 L. Wei, F. Hu, Y. Shen, Z. Chen, Y. Yu, C.-C. Lin, M. C. Wang and W. Min, *Nat. Methods*, 2014, **11**, 410–412.

- 7 M. M. Gaschler, F. Hu, H. Feng, A. Linkermann, W. Min and B. R. Stockwell, *ACS Chem. Biol.*, 2018, **13**, 1013–1020.
- 8 W. J. Tipping, M. Lee, A. Serrels, V. G. Brunton and A. N. Hulme, *Chem. Sci.*, 2017, **8**, 5606–5615.
- 9 J. Seidel, Y. Miao, W. Porterfield, W. Cai, X. Zhu, S.-J. Kim, F. Hu, S. Bhattacharai-Kline, W. Min and W. Zhang, *Chem. Commun.*, 2019, **55**, 9379–9382.
- 10 L. E. Jamieson, J. Greaves, J. A. McLellan, K. R. Munro, N. C. O. Tomkinson, L. H. Chamberlain, K. Faulds and D. Graham, *Spectrochim. Acta, Part A*, 2018, **197**, 30–36.
- 11 C. Zeng, F. Hu, R. Long and W. Min, *Analyst*, 2018, **143**, 4844–4848.
- 12 L. T. Wilson, W. J. Tipping, L. E. Jamieson, C. Wetherill, Z. Henley, K. Faulds, D. Graham, S. P. Mackay and N. C. O. Tomkinson, *Analyst*, 2020, **145**, 5289–5298.
- 13 X. Huang, J. Song, B. C. Yung, X. Huang, Y. Xiong and X. Chen, *Chem. Soc. Rev.*, 2018, **47**, 2873–2920.
- 14 L. E. Jamieson, C. Wetherill, K. Faulds and D. Graham, *Chem. Sci.*, 2018, **9**, 6935–6943.
- 15 Y. Zhou, J. F. Zhang and J. Yoon, *Chem. Rev.*, 2014, **114**, 5511–5571.
- 16 Y. Jiao, B. Zhu, J. Chen and X. Duan, *Theranostics*, 2015, **5**, 173–187.
- 17 S. Y. Kim, J. Park, M. Koh, S. B. Park and J.-I. Hong, *Chem. Commun.*, 2009, 4735–4737.
- 18 D. Kim, S. Singha, T. Wang, E. Seo, J. H. Lee, S.-J. Lee, K. H. Kim and K. H. Ahn, *Chem. Commun.*, 2012, **48**, 10243–10245.
- 19 A. Roy, D. Kand, T. Saha and P. Talukdar, *Chem. Commun.*, 2014, **50**, 5510–5513.
- 20 M. Jo, J. Lim and O. Š. Miljanic, *Org. Lett.*, 2013, **15**, 3518–3521.
- 21 L. Fu, F.-L. Jiang, D. Fortin, P. D. Harvey and Y. Liu, *Chem. Commun.*, 2011, **47**, 5503–5505.
- 22 H. Lu, Q. Wang, Z. Li, G. Lai, J. Jiang and Z. Shen, *Org. Biomol. Chem.*, 2011, **9**, 4558–4562.
- 23 D. Buckland, S. V. Bhosale and S. J. Langford, *Tetrahedron Lett.*, 2011, **52**, 1990–1992.
- 24 M. R. Rao, S. M. Mobin and M. Ravikanth, *Tetrahedron*, 2010, **66**, 1728–1734.
- 25 L. Fu, F.-F. Tian, L. Lai, Y. Liu, P. D. Harvey and F.-L. Jiang, *Sens. Actuators, B*, 2014, **193**, 701–707.
- 26 M. Kaur, M. J. Cho and D. H. Choi, *Dyes Pigm.*, 2014, **103**, 154–160.
- 27 P. Chen, W. Bai and Y. Bao, *J. Mater. Chem. C*, 2019, **7**, 11731–11746.
- 28 L. Gai, J. Mack, H. Lu, T. Nyokong, Z. Li, N. Kobayashi and Z. Shen, *Coord. Chem. Rev.*, 2015, **285**, 24–51.
- 29 G. L. Larson, *Synthesis*, 2018, 2433–2462.
- 30 N. E. Leadbeater and J. R. Schmink, *Nat. Protoc.*, 2007, **3**, 1.
- 31 W. J. Tipping, M. Lee, V. G. Brunton, G. C. Lloyd-Jones and A. N. Hulme, *Faraday Discuss.*, 2019, **220**, 71–85.
- 32 H. F. Shurvell and M. C. Southby, *Vib. Spectrosc.*, 1997, **15**, 137–146.
- 33 L. Trembleau, T. A. D. Smith and M. H. Abdelrahman, *Chem. Commun.*, 2013, **49**, 5850–5852.
- 34 X. Wu, H. Wang, S. Yang, H. Tian, Y. Liu and B. Sun, *ACS Omega*, 2019, **4**, 4918–4926.
- 35 L. C. Murfin, K. Chiang, G. T. Williams, C. L. Lyall, A. T. A. Jenkins, J. Wenk, T. D. James and S. E. Lewis, *Front. Chem.*, 2020, **8**, 10.
- 36 S. Rochat and K. Severin, *Chem. Commun.*, 2011, **47**, 4391–4393.
- 37 L. Wei, Z. Chen, L. Shi, R. Long, A. V. Anzalone, L. Zhang, F. Hu, R. Yuste, V. W. Cornish and W. Min, *Nature*, 2017, **544**, 465.
- 38 H. Matsui, M. Morimoto, K. Horimoto and Y. Nishimura, *Toxicol. In Vitro*, 2007, **21**, 1113–1120.

